



ELSEVIER

Contents lists available at ScienceDirect

## Journal of Solid State Chemistry

journal homepage: [www.elsevier.com/locate/jssc](http://www.elsevier.com/locate/jssc)

# Crystal structure and electronic properties of the new compounds $U_3Co_{12-x}X_4$ with $X=Si, Ge$

A. Soudé<sup>a</sup>, O. Tougait<sup>a,\*</sup>, M. Pasturel<sup>a</sup>, D. Kaczorowski<sup>b</sup>, H. Noël<sup>a</sup><sup>a</sup> Sciences Chimiques de Rennes, Chimie du Solide et Matériaux, Université Rennes 1, UMR CNRS 6226, 263 Avenue du Général Leclerc, 35042 Rennes, France<sup>b</sup> Institute of Low Temperature and Structure Research, Polish Academy of Sciences, ul. Okólna 2, 50-422 Wrocław, Poland

## ARTICLE INFO

## Article history:

Received 21 January 2010

Received in revised form

5 March 2010

Accepted 7 March 2010

Available online 17 March 2010

## Keywords:

Intermetallics

Single crystal X-ray diffraction

Pauli paramagnetism

## ABSTRACT

The new compounds  $U_3Co_{12-x}X_4$  with  $X=Si, Ge$  were prepared by direct solidification of the corresponding liquid phase, followed by subsequent annealing at 1173 K. Single crystal X-ray diffraction carried out at room temperature showed that they crystallize with the hexagonal space group  $P6_3/mmc$  (no.194) and the unit-cell parameters  $a=8.130(5)$ ,  $c=8.537(5)$  Å and  $a=8.256(1)$ ,  $c=8.608(1)$  Å for the silicide and germanide, respectively. Their crystal structure derives from the  $EuMg_{5.2}$  structure type, and is closely related to the  $Sc_3Ni_{11}Si_4$  and  $Gd_3Ru_{4-x}Al_{12+x}$  types. For the present compounds, no substitution mechanisms have been observed, the partial occupancy of one Co site results from the presence of vacancies, only. The homogeneity ranges, evaluated by energy dispersive spectroscopy analysis, extend from  $x=0.0(2)$  to  $0.3(2)$  and from  $x=0.0(2)$  to  $1.0(2)$  for  $U_3Co_{12-x}Si_4$  and  $U_3Co_{12-x}Ge_4$ , respectively. The electronic properties of both compounds were investigated by means of DC magnetic susceptibility and DC electrical resistivity measurements. The  $U_3Co_{12-x}X_4$  compounds are both Pauli paramagnets with their electrical resistivity best described as poor metallic or dirty metallic behavior.

© 2010 Elsevier Inc. All rights reserved.

## 1. Introduction

The binary compound  $UGe_2$  [1] and the ternary compounds  $URhGe$  [2] and  $UCoGe$  [3] are known to exhibit interesting electronic properties including ferromagnetic ordering and superconductivity. The ternary compounds show coexistence of both behaviors at ambient pressure. Unlike for conventional superconductors, theoretically described by the BCS theory [4], superconductivity in the above cited U-based materials appears to be mediated by magnetic fluctuations [5] and therefore ferromagnetic order and superconductivity should not be considered as exclusively antagonistic. The recent findings have boosted up explorative investigations of the crystal chemistry and low-temperature physical properties of new ternary phases in the U-T-X systems, where T is a transition metal and X a p-block element.

Previous studies on the U-Co-Ge system have revealed the existence of six intermetallic phases:  $UCoGe$  [6],  $UCo_2Ge_2$  [7],  $UCo_6Ge_6$  [8],  $U_3Co_2Ge_7$  [9],  $U_3Co_4Ge_7$  [10] and  $U_2Co_{17-y}Ge_y$  with  $1.3 \leq y \leq 3$  [11]. Our present study of this ternary system highlights the existence of a new compound,  $U_3Co_{12}Ge_4$ . It crystallizes with a structure related to the  $EuMg_{5.2}$ -type [12],

which can exhibit several distributions of atoms for a ternary variant, including various substitution mechanisms. In order to determine unambiguously the arrangement of the atoms in the unit-cell, the silicide counterpart,  $U_3Co_{12}Si_4$ , has also been studied. The larger difference in the atomic numbers between Co and Si, compared to Co and Ge, gives additional credit to the results of the X-ray diffraction experiments. Herein, we present the single crystal structure refinements and the electronic properties of the new compounds  $U_3Co_{12-x}X_4$  with  $X=Si, Ge$ .

## 2. Experimental details

Starting materials for the syntheses were uranium turnings, cobalt and germanium or silicon pieces (all purities above 99.9%). Calculated amounts of the components were melted in an arc-furnace under residual argon atmosphere. In order to ensure good homogeneity, the buttons were turned and re-melted. To promote homogenization and crystallization of the samples, heat treatments at high temperature were undertaken. The  $U_3Co_{12-x}X_4$  samples were annealed at 1173 K for 2 weeks in sealed silica tubes, followed by quenching down to room temperature. Single crystals suitable for crystal structure determination were selected from crushed ingots of the as-cast sample of the silicide and the heat-treated sample of the germanide.

\* Corresponding author. Fax: +33 2 23 23 67 99.

E-mail address: [tougait@univ-rennes1.fr](mailto:tougait@univ-rennes1.fr) (O. Tougait).

Scanning electron microscopy coupled with energy-dispersive spectroscopy (SEM-EDS) were performed on pieces of each sample embedded in resin and polished using SiC paper and diamond paste down to 1  $\mu\text{m}$  particle size. The compositional contrast among the various phases was revealed by means of a backscattered electron detector on a 6400-JSM scanning electron microscope and chemical analyses were obtained with an Oxford Link Isis energy-dispersive spectrometer. The precision of these measurements is considered to be about 1 at.% for U, Co and Ge and about 2 at.% for Si, when accompanied by a heavy element such as uranium ( $Z=92$ ).

The samples were examined by X-ray powder diffraction (XRD) with a Bruker AXS D8 Advance diffractometer ( $\theta$ - $2\theta$  Bragg-Brentano geometry) using monochromatized  $\text{CuK}\alpha_1$  radiation ( $\lambda=1.5406 \text{ \AA}$ ). The POWDERCELL software package [13] was used to compare the experimental diffraction patterns with those generated for the known compounds and to refine the unit-cell parameters.

Single crystal X-ray diffraction intensities were collected on a Bruker Kappa CCD four circle diffractometer working with  $\text{MoK}\alpha$  radiation ( $\lambda=0.71073 \text{ \AA}$ ). The orientation matrix and the unit-cell parameters were derived from the first ten measured frames of the data using the DENZO software [14]. The scaling and merging of redundant measurements of the different data sets as well as the cell refinement was performed using DENZO-ScalePack [15]. Semi-empirical absorption corrections were made with the use of the MULTISCAN software [16]. Structural models were determined by direct methods using SIR-97 [17]. All structure refinements and Fourier syntheses were made with the help of SHELXL-97 [18]. The atomic positions have been standardized using STRUCTURE TIDY [19].

Polycrystalline samples used for measurements of the physical properties were obtained by arc-melting the components taken with the atomic ratio of U:Co:Ge equal to 16:62.5:21.5 and U:Co:Si equal to 16:62.7:21.3. Subsequently, the buttons were heat treated at 1173 K for 24 hours to remove constraints. Analyses of both the X-ray diffraction patterns and the metallographic images revealed single phases.

DC magnetic measurements were carried out using a Quantum Design MPMS-5 SQUID magnetometer. The data were collected in the temperature range 2–300 K with applied magnetic fields up to 50 kOe. The electrical resistivity was measured over the temperature interval 4.2–300 K employing a standard DC four-point technique. The current leads (copper wires) were attached to the specimen using silver epoxy, while the voltage contacts were made by spot welding copper wires.

### 3. Results

#### 3.1. Phase formation

The existence of the new phase  $\text{U}_3\text{Co}_{12-x}\text{Ge}_4$  has been revealed during our systematic investigation of the U-Co-Ge ternary phase diagram. This compound was observed in some arc melted samples and found to be stable upon heat treatment at temperatures above 973 K. The metallographic and EDS analyses indicated a ternary phase with nominal composition U:Co:Ge of 16(1):63(1):21(1). Its X-ray powder diffraction pattern could be indexed by adjusting the hexagonal unit-cell parameters of the  $\text{EuMg}_{5.2}$  structure type. In order to confirm the crystallographic sites occupancies in  $\text{U}_3\text{Co}_{12}\text{Ge}_4$ , the silicide counterpart  $\text{U}_3\text{Co}_{12}\text{Si}_4$  has also been synthesized. Similarly to the germanide, the phase was observed in both as-cast and annealed (above 973 K) samples. The EDS analysis yielded the nominal composition U:Co:Si equal to 16(1):63(1):21(2). All the peaks on the powder X-ray

diffraction pattern could be indexed by slightly modifying the hexagonal unit-cell parameters of  $\text{U}_3\text{Co}_{12}\text{Ge}_4$ , hinting at the  $\text{EuMg}_{5.2}$  structure type.

#### 3.2. Crystal structure refinements

The relevant data concerning the single crystal X-ray diffraction data collections done for  $\text{U}_3\text{Co}_{12-x}\text{Ge}_4$  and  $\text{U}_3\text{Co}_{12-x}\text{Si}_4$  are gathered in Table 1. The systematic extinctions  $hhl, l \neq 2n$  are compatible with the hexagonal space group  $P6_3/mmc$  (no. 194) assigned for the  $\text{EuMg}_{5.2}$  type. In this structure the unique crystallographically independent europium atom is located on a 6h Wyckoff site, whereas the seven non-equivalent magnesium atoms are located on 12k, 6h, 6g, 4f, 4e, 2b and 2a Wyckoff sites. The 4e, 2b and 2a positions are filled only partially, with the site occupancies of 0.26, 0.77 and 0.40, respectively [12], yielding the crystallographic formula,  $\text{Eu}_6\text{Mg}_{31.38}$ . The single crystal hereafter labelled "A" was selected from a sample with the initial composition U:Co:Ge of 3:12:4, annealed at 1173 K. The initial structural model, resulting from phase determination by direct methods, indicated the following distribution of atoms on the Wyckoff sites: U on 6h, Co on 12k, 6h, 4f and 2b and Ge on 6g and 2a. Refinements with this initial model displayed some excess of the electronic density in the vicinity of the 2b site occupied by the  $\text{Co}_4$  atom, hence suggesting that this position is only partially occupied. In subsequent refinements, the occupancy level of the 2b site got reduced to a value around 2/3. Additional cycles of refinement, performed with the  $\text{Ge}_2$  atom located on the 2a site (0, 0, 0), yielded a maximum residual electron density of about 8.71 electrons per  $\text{\AA}^3$ , at 0.39  $\text{\AA}$  out of the  $\text{Ge}_2$  site, which is a value rather high for a ternary U-based compound. In addition to this residual peak in the Fourier map, the anisotropic displacement parameters of the  $\text{Ge}_2$  atom were found abnormally elongated

**Table 1**

Single crystal X-ray diffraction data and structure refinement results for  $\text{U}_3\text{Co}_{12-x}\text{Ge}_4$  and  $\text{U}_3\text{Co}_{12-x}\text{Si}_4$

Crystal label	A	B
Crystallographic formula	$\text{U}_6\text{Co}_{23.32}\text{Ge}_8$	$\text{U}_6\text{Co}_{23.5}\text{Si}_8$
Molecular weight ( $\text{g mol}^{-1}$ )	3423.22	3067.22
Crystal system, Space group	Hexagonal, $P6_3/mmc$ (no. 194)	Hexagonal, $P6_3/mmc$ (no. 194)
Lattice parameters ( $\text{\AA}$ )	$a=8.256(1) \text{ \AA}$ $c=8.608(1) \text{ \AA}$	$a=8.130(5) \text{ \AA}$ $c=8.537(5) \text{ \AA}$
Volume ( $\text{\AA}^3$ )	508.08(2)	488.7(5)
Z, Density calculated ( $\text{g cm}^{-3}$ )	1/11.19	1/10.42
Absorption coefficient ( $\text{mm}^{-1}$ )	78.2	69.7
Crystal size ( $\text{mm}^3$ )	$0.034 \times 0.027 \times 0.010$	$0.060 \times 0.040 \times 0.040$
Crystal colour	Black	Black
$\theta$ range ( $^\circ$ )	3.70–42.11	3.75–41.99
$hkl$ range	$-15 < h < 9$ $-12 < k < 15$ $-16 < l < 15$	$-8 < h < 15$ $-15 < k < 15$ $-16 < l < 15$
Reflexions collected/ unique	11713/719	15851/687
Absorption correction	Semi-empirical (MULTISCAN)	Semi-empirical (MULTISCAN)
Max/min transmissions	0.2761/0.1347	0.1650/0.0327
$R(\text{int})$	0.0816	0.1020
Refined parameters	30	30
G.O.F	1.113	1.206
$wR_2 [I > 2\sigma(I)]$	0.0691	0.0804
$R_1 [I > 2\sigma(I)]$	0.0297	0.0371
Extinction coefficient	0.0029	0.0018
Residual peaks ( $\text{e \AA}^{-3}$ )	3.273/–3.832	5.177/–2.737

along the  $c$  direction (Fig. 1a). Therefore, subsequent refinements have been performed with the  $\text{Ge}_2$  atom positioned at a  $4e$  site  $(0, 0, z)$  with  $z \approx 0.03$  and with a free occupancy parameter, as it is possible for the  $\text{EuMg}_{5.2}$ -type structure (see above). The refinement converged to 50% occupancy of this site, with a significant reduction in the reliability factors, viz.  $R_1=0.0297$  and  $wR_2=0.0691$  compared to  $R_1=0.0335$  and  $wR_2=0.0833$  for the model with  $\text{Ge}_2$  located at the  $2a$  site. Furthermore, the resulting anisotropic displacements of  $\text{Ge}_2$  at the  $4e$  site were similar to those of the other atoms in the asymmetric unit (Fig. 1b). The maximum residual electron density, located near the  $\text{Co}_2$  site, reached a low value of 3.27 electrons per  $\text{\AA}^3$ , which is usually observed for U-based compounds with unit-cell volume similar to that of  $\text{U}_3\text{Co}_{12-x}\text{Ge}_4$  [20,21]. The chemical formula deduced from the crystallographic analysis is  $\text{U}_3\text{Co}_{11.66}\text{Ge}_4$  which perfectly matches the result of our methodical microprobe experiments that reveal a small deficit on the cobalt sublattice, indicating that  $\text{U}_3\text{Co}_{12-x}\text{Ge}_4$  has a homogeneity domain  $0.0(2) < x < 1.0(2)$ . The careful analysis of the experimental points issued from various samples indicates that the atomic composition of the limits of the homogeneity domain evolve within the U:Co:Ge atomic ratio of 16:63:21 to 17:61:22, which correspond to the chemical formulae of  $\text{U}_3\text{Co}_{12}\text{Ge}_4$  and  $\text{U}_3\text{Co}_{11}\text{Ge}_4$ , respectively. Additionally, small

reductions, of few hundredths of Angström, of the unit-cell parameters  $a$  and  $c$  are observed for  $\text{U}_3\text{Co}_{11}\text{Ge}_4$  compared to  $\text{U}_3\text{Co}_{12}\text{Ge}_4$ .

The single crystal hereafter labelled “B” was selected from an as-cast sample having an initial composition U:Co:Si of 3:11:4. The silicide has only slightly smaller lattice parameters,  $a=8.130(5)$  and  $c=8.537(5)\text{\AA}$ , than those of the germanide. The initial atomic positions for the crystallographic refinement were taken from crystal A. The calculations converged to low reliability factors for the model with partial occupation of about 3/4 of the  $\text{Co}_4$  site and with the  $\text{Si}_2$  atom located on the  $4e$  site  $(0, 0, z)$  with  $z \approx 0.02$ . The final Fourier map was featureless, and the anisotropic displacement parameters for all the atoms had reasonable values. Nevertheless, the structural model with a mutual substitution of Co and Si atoms on the  $2b$  Wyckoff site was also tested, providing a 50%:50% occupation factor. The corresponding chemical formula was significantly distinguishable from the one assessed from the elemental analysis, hence indicating that only the partial occupation on the  $2b$  site by a Co atom has to be considered. Within this scenario, the chemical composition  $\text{U}_3\text{Co}_{11.75}\text{Si}_4$  is obtained, in good agreement with the formula deduced from the methodical microprobe analysis. This result implies a small deficit of Co around the ideal composition. Apparently,  $\text{U}_3\text{Co}_{12-x}\text{Si}_4$  is a solid solution with vacancies on the Co sublattice, quantified by the homogeneity domain  $0.0(2) < x < 0.3(2)$ . The lower limit of the homogeneity range matches quite well the chemical formula deduced from the single crystal XRD refinement.

The detailed crystallographic investigation supplemented with the careful chemical analyses confirmed that  $\text{U}_3\text{Co}_{12-x}\text{Ge}_4$  and  $\text{U}_3\text{Co}_{12-x}\text{Si}_4$  are isostructural and crystallize in a ternary substitution derivative of the  $\text{EuMg}_{5.2}$ -type structure, as previously encountered for the  $\text{Sc}_3\text{Ni}_{11}\text{Si}_4$ -type [22] and  $\text{Gd}_3\text{Ru}_{4+x}\text{Al}_{12-x}$ -type [23]. The atomic positional and displacement parameters and the interatomic distances for both investigated compounds are listed in Tables 2 and 3, respectively. In the latter table, the shortest distances involving the  $\text{Ge}_2$  and  $\text{Si}_2$  atoms generated by the  $3m$  symmetry of the  $4e$  site are skipped.

### 3.3. Crystal structure description

The structure of  $\text{U}_3\text{Co}_{12-x}\text{Si}_4$  can be described as a stacking of U-Co and Co-Si layers, which alternate along the  $c$ -axis. The U-Co layer (Fig. 2) is composed of U atoms forming a distorted Kagomé network, with one Co atom inserted in large  $[\text{U}_3]$  triangles, empty small  $[\text{U}_3]$  triangles, and three cobalt atoms positioned within the  $[\text{U}_6]$  hexagons. The shortest distances between U atoms, within small triangles, are  $3.613(1)\text{\AA}$  (Table 3), i.e. above the Hill limit of  $3.5\text{\AA}$ , which delimits the spacing for the overlap of the  $5f$  wavefunctions [24]. The non-planar Co-Si layer can be described as a network of cobalt atoms forming “chair” like configuration of  $[\text{Co}_6]$  hexagons centred by Si (Fig. 3a and b).

For both compounds  $\text{U}_3\text{Co}_{12-x}\text{Ge}_4$  and  $\text{U}_3\text{Co}_{12-x}\text{Si}_4$ , the distances between  $\text{Co}_4$  and  $\text{X}_2$  atoms along the  $c$ -axis,  $d(\text{Ge}_2\text{-Co}_4)=2.380(1)$  and  $d(\text{Co}_4\text{-Si}_4)=2.306(1)\text{\AA}$ , are shorter than the sums of the metallic and covalent radii of the corresponding elements ( $r_{\text{Co}}+r_{\text{Ge}}=2.48\text{\AA}$ ) and ( $r_{\text{Co}}+r_{\text{Si}}=2.43\text{\AA}$ ) [25]. This is due to the stacking default on the Co sublattice, established in the crystallographic investigations. Roughly 1/3 in the case of the germanide and 1/4 in the case of the silicide of the  $\text{Co}_4$  atoms are missing. The presence of these vacancies allows some diffusion process in the crystals, and the  $\text{X}_2$  atoms may change their positions along the  $c$ -direction, if the nearby  $\text{Co}_4$  site is empty. The resulting arrangement of the atoms yields an average model of the crystal structure, with no definitive physical meaning of the so-derived interatomic  $\text{Co}_4\text{-X}_2$  distances.

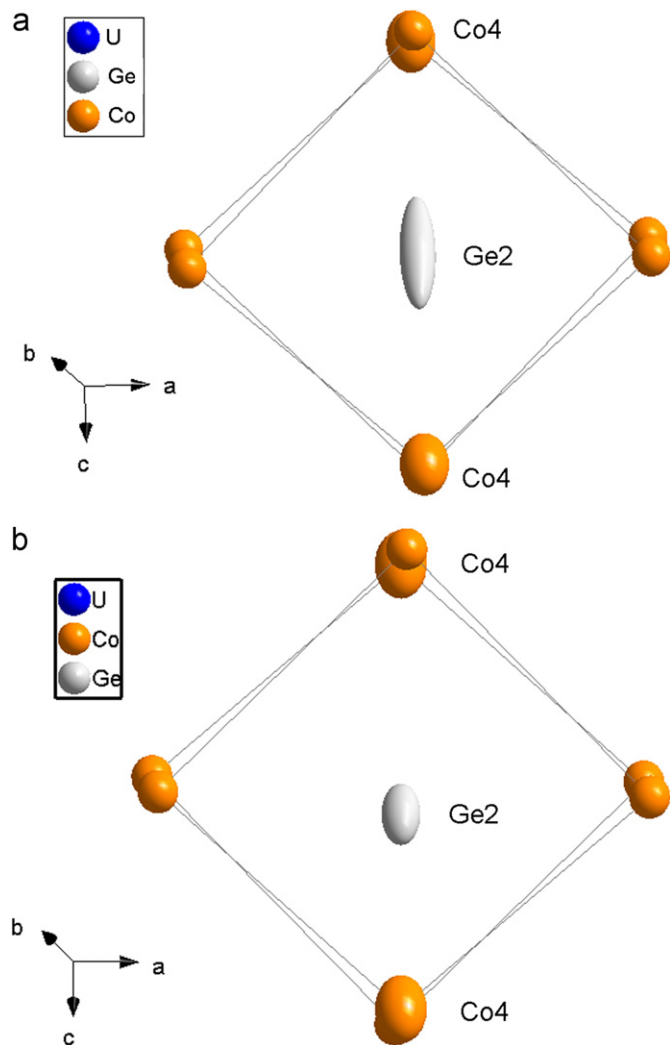


**Fig. 1.** View of the  $\text{Ge}_2$  coordination sphere with the principal mean square atomic displacement parameters with the hypothesis of (a) a full occupation of the  $2a$  site and (b) a half-occupation of the  $4e$  site. The displacement ellipsoids are drawn with 75% probability level.

**Table 2**

Atomic positions, occupancy rates and atomic displacement parameters for (a)  $U_3Co_{12-x}Ge_4$  and (b)  $U_3Co_{12-x}Si_4$ . Atomic positions were standardized using the Structure Tidy software [19].

Atom	Wyck.	Occ.	x	y	z	$U_{eq}(\text{Å}^2)$
<b>(a)</b>						
U <sub>1</sub>	6h	1.0	0.1875(1)	2x	1/4	0.0130(1)
Co <sub>1</sub>	12k	1.0	0.1620(1)	2x	0.5949(1)	0.0124(1)
Co <sub>2</sub>	6h	1.0	0.5653(1)	2x	1/4	0.0110(2)
Co <sub>3</sub>	4f	1.0	1/3	2/3	0.0045(1)	0.0125(2)
Co <sub>4</sub>	2b	0.66(1)	0	0	1/4	0.026(1)
Ge <sub>1</sub>	6g	1.0	1/2	0	0	0.0110(1)
Ge <sub>2</sub>	4e	0.50(1)	0	0	0.031(3)	0.0182(8)
<b>(b)</b>						
U <sub>1</sub>	6h	1.0	0.1893(3)	2x	1/4	0.0115(1)
Co <sub>1</sub>	12k	1.0	0.1620(1)	2x	0.5912(1)	0.0116(2)
Co <sub>2</sub>	6h	1.0	0.5624(1)	2x	1/4	0.0131(3)
Co <sub>3</sub>	4f	1.0	1/3	2/3	0.0074(3)	0.0116(3)
Co <sub>4</sub>	2b	0.75(2)	0	0	1/4	0.023(1)
Si <sub>1</sub>	6g	1.0	1/2	0	0	0.0105(5)
Si <sub>2</sub>	4e	0.50(2)	0	0	0.020(3)	0.014(5)

**Table 3**

Selected interatomic distances for  $U_3Co_{12-x}Ge_4$  and  $U_3Co_{12-x}Si_4$ .

	$U_3Co_{12}Ge_4$ (A)		$U_3Co_{12}Si_4$ (B)	
U <sub>1</sub>	1 Co <sub>4</sub>	2.680(1)	1 Co <sub>4</sub>	2.665(2)
	4 Co <sub>1</sub>	2.850(1)	2 Co <sub>2</sub>	2.824(2)
	2 Co <sub>2</sub>	2.904(1)	4 Co <sub>1</sub>	2.838(2)
	2 Co <sub>3</sub>	2.970(1)	2 Co <sub>3</sub>	2.899(2)
Co <sub>1</sub>	2 Co <sub>1</sub>	2.991(1)	2 Co <sub>1</sub>	2.939(2)
	4 Ge <sub>1</sub>	3.113(1)	4 Si <sub>1</sub>	3.069(1)
	2 Co <sub>2</sub>	2.518(1)	1 Si <sub>2</sub>	2.47(1)
	1 Ge <sub>1</sub>	2.552(1)	2 Si <sub>1</sub>	2.507(2)
Co <sub>2</sub>	1 Ge <sub>2</sub>	2.556(1)	2 Co <sub>2</sub>	2.508(2)
	1 Co <sub>3</sub>	2.595(1)	1 Co <sub>3</sub>	2.560(2)
	1 Co <sub>1</sub>	2.672(2)	1 Co <sub>4</sub>	2.649(2)
	1 Co <sub>4</sub>	2.673(1)	1 Co <sub>1</sub>	2.712(3)
	2 Co <sub>1</sub>	2.833(2)	2 Co <sub>1</sub>	2.758(2)
	2 U <sub>1</sub>	2.850(1)	2 U <sub>1</sub>	2.838(2)
	1 U <sub>1</sub>	2.991(1)		
Co <sub>3</sub>	2 Ge <sub>1</sub>	2.346(1)	2 Si <sub>1</sub>	2.308(1)
	2 Co <sub>2</sub>	2.511(2)	4 Co <sub>1</sub>	2.508(2)
	4 Co <sub>1</sub>	2.518(1)	2 Co <sub>2</sub>	2.543(3)
	2 Co <sub>3</sub>	2.626(1)	2 Co <sub>3</sub>	2.643(2)
Co <sub>4</sub>	2 U <sub>1</sub>	2.904(1)	2 U <sub>1</sub>	2.824(2)
	3 Ge <sub>2</sub>	2.384(1)	3 Si <sub>2</sub>	2.348(2)
	3 Co <sub>1</sub>	2.595(1)	3 Co <sub>1</sub>	2.560(2)
	3 Co <sub>2</sub>	2.626(1)	3 Co <sub>2</sub>	2.643(2)
X <sub>1</sub>	3 U <sub>1</sub>	2.970(1)	3 U <sub>1</sub>	2.899(2)
	2 Ge <sub>2</sub>	2.418(3)	2 Si <sub>2</sub>	2.31(3)
	6 Co <sub>1</sub>	2.673(1)	6 Co <sub>1</sub>	2.649(2)
X <sub>2</sub>	3 U <sub>1</sub>	2.680(1)	3 U <sub>1</sub>	2.665(2)
	2 Co <sub>2</sub>	2.346(1)	2 Co <sub>2</sub>	2.308(1)
	2 Co <sub>3</sub>	2.384(1)	2 Co <sub>3</sub>	2.348(1)
X <sub>2</sub>	4 Co <sub>1</sub>	2.552(1)	4 Co <sub>1</sub>	2.507(2)
	4 U <sub>1</sub>	3.113(1)	4 U <sub>1</sub>	3.069(1)
	3 Co <sub>1</sub>	2.380(1)	1 Co <sub>4</sub>	2.31(3)
X <sub>2</sub>	1 Co <sub>4</sub>	2.418(3)	3 Co <sub>1</sub>	2.356(7)
	3 Co <sub>1</sub>	2.556(1)	3 Co <sub>1</sub>	2.47(1)

The three types of structures,  $Sc_3Ni_{11}Si_4$ ,  $Gd_3Ru_{4+x}Al_{12-x}$  and  $U_3Co_{12-x}X_4$ , appear to be ternary substitution derivatives of the  $EuMg_{5.2}$ -type. In all these structures, the *f*-elements (including Sc) are located at the 6h site, with full occupancy. They form a distorted Kagomé network resulting from vertex-sharing of small and large triangles. The network of triangles also defines the hexagons, inside

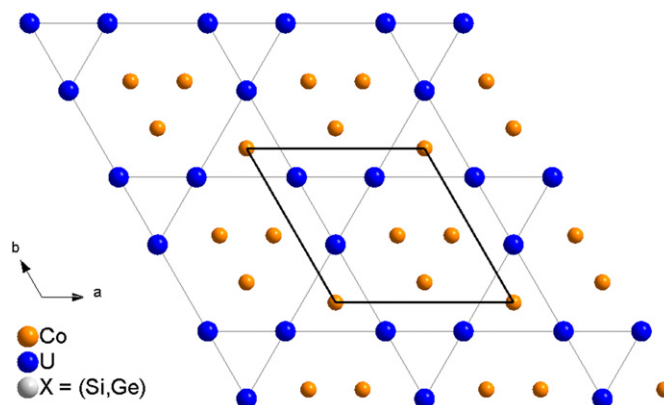


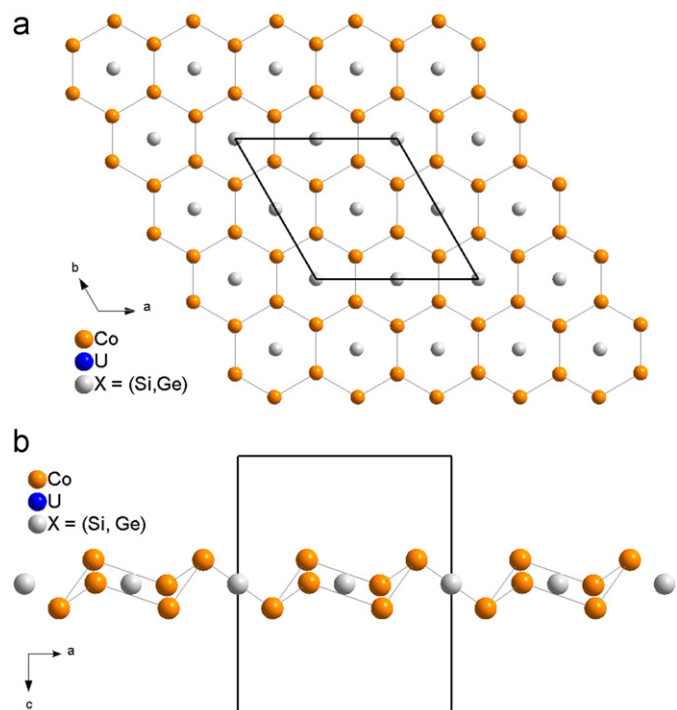
**Fig. 2.** View of the U-Co layer of the  $U_3Co_{12-x}Si_4$  structure showing the distorted U-Kagomé network with insertion of Co atoms.

which the atoms are placed at the other 6h position. This site is also fully occupied, with a mixed occupancy Ru/Al in the case of  $Gd_3Ru_{4+x}Al_{12-x}$ . The large triangles are centered by an element lying on the 2b site, whereas the small triangles remain empty. The 2b Wyckoff sites are fully occupied in the case of  $Sc_3Ni_{11}Si_4$  and  $Gd_3Ru_{4+x}Al_{12-x}$ , whereas they are only partially occupied in the case of  $EuMg_{5.2}$  and  $U_3Co_{12-x}X_4$ . The main difference between the considered structures regards the occupancy of the 2a or 4e sites. Both of these sites are empty in  $Sc_3Ni_{11}Si_4$ , whereas they are both partially occupied in  $EuMg_{5.2}$ . Only the 2a site is occupied in the case of  $Gd_3Ru_{4+x}Al_{12-x}$ , and only the 4e site is partially occupied, in  $U_3Co_{12-x}X_4$ . It seems that the atom filling in these two positions is directly linked to the occupancy of the 2b site. When the 2b site is fully occupied, there is no disorder between the 2a or 4e sites, as it is the case for  $Sc_3Ni_{11}Ge_4$  and  $Gd_3Ru_{4+x}Al_{12-x}$ . In turn, when the 2b site is partially occupied, leading to vacancies, a diffusion process appears along the [0 0 1] direction, affecting the occupancy of the 2a and 4e positions.

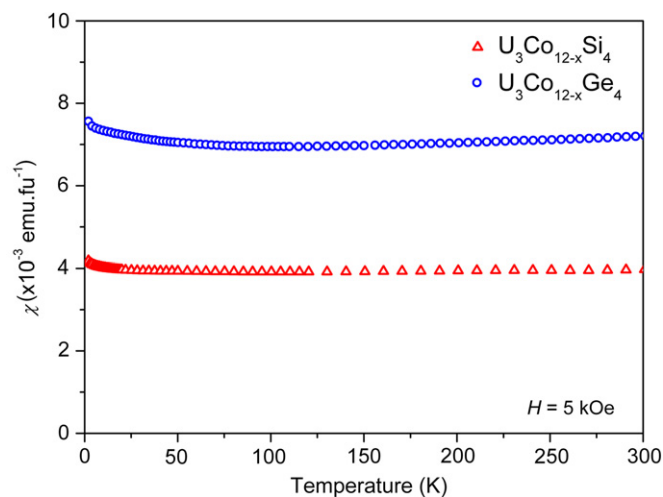
### 3.3. Magnetic and electrical properties

Fig. 4 presents the temperature dependencies of the molar magnetic susceptibility,  $\chi(T)$ , of  $U_3Co_{12-x}Ge_4$  with  $x=0.34(2)$  and  $U_3Co_{12-x}Si_4$  with  $x=0.25(2)$ . Both compounds are Pauli





**Fig. 3.** (a) Top view of Co-Si layer of the  $U_3Co_{12-x}Si_4$  structure composed of Co hexagons centred by Si atoms and (b) lateral view of this non-planar Co-Si layer which adopt a chair-like configuration.



**Fig. 4.** Temperature variations of the molar magnetic susceptibility of  $U_3Co_{12-x}Ge_4$  (circles) and  $U_3Co_{12-x}Si_4$  (triangles), measured in an applied magnetic field of 5 kOe.

paramagnets with the magnetic susceptibility of about  $7.2 \times 10^{-3}$  and  $4.0 \times 10^{-3} \text{ emu mol}^{-1}$  at room temperature, respectively. The magnetization isotherms taken at 2 K, displayed in Fig. 5, are linear and fully reversible when measured with increasing and decreasing magnetic field. The non-magnetic character of both compounds likely results from strong hybridization of the uranium 5f electronic states with the 3d states of the cobalt atoms.

The temperature variations of the electrical resistivity of  $U_3Co_{12-x}Ge_4$  and  $U_3Co_{12-x}Si_4$  are shown in Fig. 6. The germanide exhibits a metallic character of the electronic transport, with strongly curvilinear  $\rho(T)$  dependence. This latter feature hints at significant contribution of spin fluctuations,

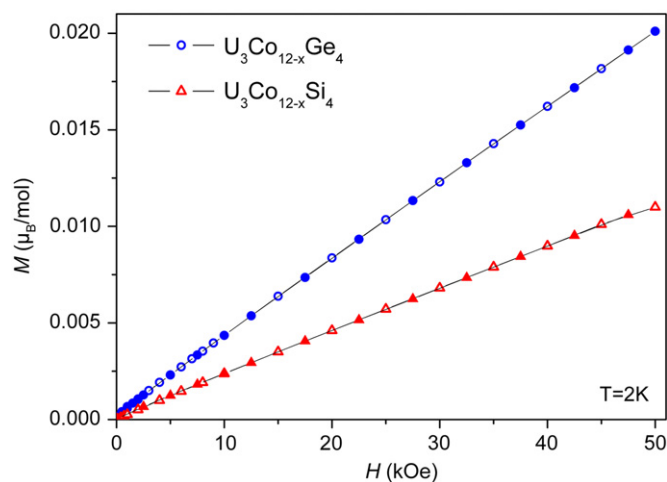


**Fig. 5.** Magnetization isotherms of  $U_3Co_{12-x}Ge_4$  and  $U_3Co_{12-x}Si_4$ , taken at 2 K with increasing (full symbols) and decreasing (open symbols) magnetic field.

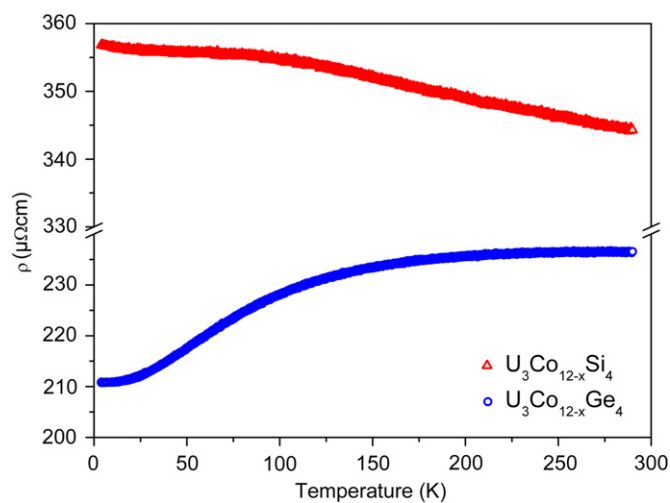


**Fig. 6.** Temperature dependence of the electrical resistivity of  $U_3Co_{12-x}Ge_4$  (circles) and  $U_3Co_{12-x}Si_4$  (triangles).

which may primarily be associated with the cobalt 3d shell. In contrast, the resistivity of  $U_3Co_{12-x}Si_4$  slightly increases with decreasing temperature, in a manner characteristic of strongly disordered metals. In this context it is worth noting the rather large value of  $344(1) \mu\Omega\text{cm}$  of the resistivity at room temperature, which rises to  $357(1) \mu\Omega\text{cm}$  at liquid helium temperature. Apparently, the observed behavior should be attributed to intrinsic atomic disorder in the unit cell of the compound (see Section 3.2). Interestingly, very similar level of disorder is present in the Ge-based counterpart, and the electrical resistivity of  $U_3Co_{12-x}Ge_4$  is also rather large ( $235(1)$  and  $211(1) \mu\Omega\text{cm}$  at room and liquid helium temperature, respectively), yet nevertheless the latter compound behaves metal-like. This striking dissimilarity in the electronic transport of the two ternaries may result from subtle differences in their electronic structures in the vicinity of the Fermi energy.

#### 4. Conclusion

The new compound  $U_3Co_{12-x}Ge_4$  was discovered during the systematic investigation of the phase equilibria in the U-Co-Ge

ternary system and  $U_3Co_{12-x}Si_4$  was discovered by isotopy. Microprobe analyses revealed that these compounds have homogeneity ranges  $0.0(2) \leq x \leq 1.0(2)$  for the germanide and  $0.0(2) \leq x \leq 0.3(2)$  for the silicide. The identity of the phase was established by single crystal X-ray diffraction. The  $U_3Co_{12-x}X_4$  isotopic compounds crystallize in the hexagonal space group  $P6_3/mmc$  with lattice parameters  $a=8.256(1)$  and  $c=8.608(1)$  Å for the germanide and  $a=8.130(5)$  and  $c=8.537(5)$  Å for the silicide at room temperature. The structural model derives from the  $EuMg_{5.2}$  structure type. The crystal structure is composed of two kinds of layers. The first is constituted of U atoms forming a distorted Kagomé network, with one Co atom inserted in large triangles, empty small triangles, and three cobalt atoms positioned within the hexagons. Vacancies are observed for the Co atoms of large triangles. The second is constituted of Co chair like hexagons centred by a X atom. The magnetic measurements show Pauli paramagnetic behavior for both compounds with a magnetic susceptibility of about  $7.5 \times 10^{-3} \text{ emu mol}^{-1}$  for  $U_3Co_{12-x}Ge_4$  and  $4.0 \times 10^{-3} \text{ emu mol}^{-1}$  for  $U_3Co_{12-x}Si_4$ , at room temperature. This behavior is due to the hybridization of the uranium 5f electronic states with the 3d states of the cobalt atoms. The electrical resistivity of  $U_3Co_{12-x}Ge_4$  shows a metallic character with the presence of spin fluctuations.  $U_3Co_{12-x}Si_4$  exhibits a strongly disordered metal behavior.

#### Acknowledgments

This work was partially supported by the French–Polish Integrated Activity Program “POLONIUM” no. 20080PM (2008–2009). The authors acknowledge the use made of the Nonius Kappa CCD diffractometer through the Centre de Diffraction X (CDIFX) managed by T. Roisnel. We also thank I. Peron and F. Gouttefangeas, from the Centre de Microscopie Électronique à Balayage et microAnalyse (CMEBA). Finally, we thank Darek Badurski for electrical resistivity measurements.

#### Appendix A. Supplementary material

Supplementary data associated with this article can be found in the online version at doi:10.1016/j.jssc.2010.03.015.

#### References

- [1] S.S. Saxena, P. Agarwal, K. Ahilan, F.M. Grosche, R.K.W. Haselwimmer, M.J. Steiner, E. Pugh, I.R. Walker, S.R. Julian, P. Monthoux, G.G. Lonzarich, A. Huxley, I. Sheikin, D. Braithwaite, J. Flouquet, *Nature* 406 (2000) 587–592.
- [2] D. Aoki, A. Huxley, E. Ressouche, D. Braithwaite, J. Flouquet, J.P. Brison, E. Lhotel, C. Paulsen, *Nature* 413 (2001) 613–616.
- [3] N.T. Huy, A. Gasparini, D.E. de Nijs, Y. Huang, J.C.P. Gortenmulder, A. De Visser, A. Hamann, T. Görlach, H.v. Löhneysen, *Phys. Rev. Lett.* 99 (2007) 067006–1–067006–4.
- [4] J. Bardeen, L.N. Cooper, J.R. Schrieffer, *Phys. Rev.* 108 (1957) 1175–1204.
- [5] G.G. Lonzarich, in: M. Springford (Ed.), *Electron: A Centenary Volume*, Cambridge University Press, Cambridge, 1997 Chapter 6.
- [6] R. Troć, V.H. Tran, J. Magn. Mater. 73 (1988) 389–397.
- [7] T. Endstra, G.J. Nieuwenhuys, A.A. Menovsky, J.A. Mydosh, *J. Appl. Phys.* 69 (8) (1994) 4816–4818.
- [8] W. Buchholz, H.-U. Schuster, *Z. Anorg. Allg. Chem.* 482 (1981) 40–48.
- [9] S. Bobev, E.D. Bauer, F. Ronning, J.D. Thompson, J.L. Sarrao, *J. Solid State Chem.* 180 (2007) 2830–2837.
- [10] R. Pöttgen, B. Chevalier, P. Gravereau, B. Darriet, W. Jeitschko, J. Etourneau, *J. Solid State Chem.* 115 (1995) 247–254.
- [11] B. Chevalier, P. Gravereau, T. Berleureau, L. Fournès, J. Etourneau, *J. Alloys Compd.* 233 (1996) 174–182.
- [12] J. Erassme, H. Lueken, *Acta Crystallogr. B* 43 (1987) 244–250.
- [13] W. Kraus, G. Nolze, *PowderCell for Windows v. 2.4*, Federal Institute for Materials Research and Testing, Berlin, Germany, 2000.
- [14] Bruker-AXS, In: Collect, Denzo, Scalepack, Sortav. Kappa CCD Program Package, Delft, The Netherlands, 1998.
- [15] Z. Otwinowski, W. Minor, *Processing of X-ray diffraction data collected in oscillation mode, methods in enzymology*, in: C.W. Carter Jr., R.M. Sweet (Eds.), *Macromolecular Crystallography, part A, Vol. 276*, Academic Press, 1997, pp. 307–326.
- [16] R.H. Blessing, *Acta Crystallogr. A* 51 (1995) 33–38.
- [17] A. Altomare, M.C. Burla, M. Camalli, G.L. Cascarano, C. Giacovazzo, A. Guagliardi, A.G.G. Moliterni, G. Polidori, R.J. Spagna, *J. Appl. Crystallogr.* 32 (1999) 115–119.
- [18] G.M. Sheldrick, SHELXS-97 and SHELXL-97. Programs for Structure Solution and Refinement, University of Göttingen, Germany, 1997.
- [19] E. Parthé, K. Cenzual, R. Gladyshevskii, *J. Alloys Compd.* 197 (1993) 291–301.
- [20] O. Tougait, H. Noël, R. Troć, *J. Solid State Chem.* 177 (2004) 2053–2057.
- [21] D. Berthebaud, O. Tougait, M. Potel, E.B. Lopes, A.P. Gonçalves, H. Noël, *J. Solid State Chem.* 180 (2007) 2926–2932.
- [22] B.Y. Kotur, M. Sikiritsa, O.I. Bodak, E.I. Gladyshevskii, *Sov. Phys. Crystallogr.* 28 (1983) 387–389.
- [23] R.E. Gladyshevskii, O.R. Strusievicz, K. Cenzual, E. Parthé, *Acta Crystallogr. B* 49 (1993) 474–478.
- [24] H.H. Hill, in: W.N. Miner (Ed.), *Plutonium and Other Actinides*, AIME, New York, 1970.
- [25] E. Teatum, K. Gschneidner, J. Waber, *Compilation of calculated data useful in predicting metallurgical behaviour of the elements in binary alloy systems*, Los Alamos Scientific Laboratory, LA-2345, 1960.